CHRONIC TOXICITY OF GRAPHENE AND GRAPHENE OXIDE IN SEQUENCING BATCH BIOREACTORS: A COMPARATIVE INVESTIGATION

Hang N. Nguyen[1], Debora F. Rodrigues[1*]

[1] Department of Civil and Environmental Engineering, Room N136 Engineering Building 1, University of Houston, TX 77204-4003 (U.S.A.)
[1*]Corresponding Authors: Email: dfrigirodrigues@uh.edu; Phone: +1-713-743-1495

Abstract

The present study investigates the chronic toxicity of graphene (G) and graphene oxide (GO) in activated sludge. Sequencing batch bioreactors were fed with influents containing 0, 1 and 5 mg L^{-1} of GO or G (12 h cycles) for ten days. Reduction in performance of the bioreactors in relation to chemical oxygen demand, ammonia and phosphate removals was observed after three days in the bioreactors fed with 5 mg L^{-1} of nanomaterials. After about eight days, these reactors reached a steady state nutrient removal, which corresponded to recovery of certain groups of ammonia oxidizing bacteria and phosphate accumulating bacteria despite the increasing accumulation of nanomaterials in the sludge. These results suggested that biological treatment can be affected transiently by initial exposure to the nanomaterials, but certain groups of microorganisms, less sensitive to these nanomaterials, can potentially strive in the presence of these nanomaterials. Results of 16S rRNA gene deep sequencing showed that G and GO affected differently the microbial communities in the activated sludge. Between the two nanomaterials investigated, GO presented the highest impact in nutrient removal, gene abundance and changes in microbial population structures.

Key words: graphene, graphene oxide, activated sludge, ammonium monooxygenase, microbial communities

1. Introduction

Recently, graphene-based nanomaterials have been intensively used due to the unique characteristics and broad applications of these materials in different fields, such as water and wastewater treatment, medical devices, electronic and aerospace [1-3]. The global market of these nanomaterials is expected to grow and reach up $986.7 million dollars over the next 5 years [4]. A study by Lazareva & Keller estimated, based on nanomaterial production data of 2010, that the presence of carbon nanotubes, a graphene-based nanomaterial, in the wastewater treatment plants of New York City would be around 1.5 mg Kg^{-1} and 0.2 μg L^{-1} per year in biosolids and treated effluents, respectively [5]. These results showed that this carbon-based nanomaterial will tend to be retained in biosolids. In this study, Keller's group did not examine graphene or graphene oxide productions and releases, but if GO and G follow the same trends as carbon nanotubes, these nanomaterials will also end up accumulating in the sludge over time.

In previous studies, the impact of carbon-based nanomaterials in wastewater treatment has been investigated mostly in very high concentrations and for one or three days as acute toxicity assays [6-9]. These studies aimed to simulate worse case scenarios in case of industrial spills. These nanomaterials, however, will most likely be introduced in the wastewater treatment plants in much smaller concentrations than the ones previously investigated since the release of nanomaterials will be the result of direct consumption and disposal, as well as wear and tear of products containing CNTs, graphene or graphene oxide. Hence, in this study, we aim to simulate the entrance and accumulation over time of GO and G in the wastewater influent when introduced in smaller and more realistic amounts. We hypothesize that G, which is more hydrophobic and prone to aggregation in aqueous environment, will interact and accumulate more in the sludge than GO. We also hypothesize that accumulation of the GO and G in the

sludge will eventually hinder the biological treatment process due to the antimicrobial properties of these nanomaterials. To investigate these hypotheses, bioreactors were set up, which were fed with low concentrations of graphene and graphene oxide in the influent for up to 10 days. Through these ten days, we monitored the performance of the reactors by investigating chemical oxygen demand, microbial metabolic activity, nitrogen and phosphate removals, as well as gene abundances for ammonia oxidizing bacteria (AOB), phosphate accumulating microorganisms (PAO) and ammonium monooxygenase (*amoA*) genes. The changes in microbial diversity structure and abundance were also determined using the 16S rRNA gene deep sequencing technique. We also monitored the release of these nanomaterials in the effluents using a previously published technique [10]. Through mass balance, we determined the accumulation of these nanomaterials in the sludge over time.

2. Materials and methods

2.1. Preparation of graphene, graphene oxide and activated sludge batch reactors with continuous feeding of nanomaterials

The graphene (G) was purchased from XG Science (U.S.A.) and graphene oxide (GO) was synthesized following the modified Hummer's method [11]. The characterizations of G and GO can be found in supporting information (Figure S1) and in our previous studies [12, 13]. Suspension stocks for G and GO were prepared at 1000 mg L^{-1} using probe sonication for 5 min prior to use (30 kHz, Tekmar sonic disruptor, U.S.A). The stock solutions were diluted at 1 and 5 mg L^{-1} using sterile synthetic wastewater (SWW) prior to use.

All the reactors were set up with activated sludge freshly collected from the aeration basin from the Sims South Bayou Wastewater Treatment Plant (Houston, TX. USA). The reactors were fed with SWW (Table S1) with or without the nanomaterials every 12 h. Detailed information about the components of the reactor, reactor set-up and the SWW preparation procedure can be found in the supporting information. Briefly, a total of five reactors were set up in triplicate with the acclimated sludge. The experimental design included control reactors (without nanomaterials) and reactors continuously fed with 1 or 5 mg L^{-1} of G or 1 or 5 mg L^{-1} of GO. All reactors followed the same 12 h cycle as the control reactors. For analysis in each cycle, a volume of 500 mL of effluent was taken and a volume of 500 mL SWW, with or without nanomaterials, was added as influent to the reactor. Each reactor received in each cycle the same influent concentration of nanomaterial that was used at the initial reactor set up. The results of the triplicate reactors were averaged and their standard deviations were calculated.

2.2. Analysis of chemical parameters

At each cycle, the effluent of each reactor was analyzed for the following nutrient removals: ammonia (NH_3-N), nitrate (NO_3 -N), phosphate (PO_4^{3-}) and chemical oxygen demand (COD).

Effluent and influent were collected and filtered through 0.2 µm sterile syringe filters (Corning, U.S.A). Ammonia and nitrate were analyzed using Orion Dual Star benchtop equipped with Orion™ High-Performance Ammonia Electrode and Orion™ Nitrate Electrodes (Thermo Scientific). Hach kits were used to measure phosphate and COD with a spectrophotometer DR3900 (Hach, U.S.A). All the results were expressed as days running the reactor versus concentrations measured (mg L^{-1}). Metabolic activity of the microbes in activated sludge was also investigated using Vibrant Cell Metabolic Assay kit (Invitrogen) (see supporting information).

2.3. DNA extraction and real time PCR (RT-PCR)

Activated sludge samples were collected at 0, 2, 4, 6, 8 and 10 days. Amounts of 0.5 g of settled activated sludge were collected for DNA extraction with the PowerWater DNA isolation kit (Mobio, U.S.A.). All DNA samples were investigated with RT-PCR for three genes, namely: ammonia oxidizing bacteria (AOB), monooxygenase ammonia bacteria (*amoA*) and phosphate accumulation organisms (PAO). The analyses of the abundances of the genes were determined using standard curves with serial dilutions of known concentrations of the genes cloned into a plasmid provided by the TOPO TA cloning kit (Invitrogen). Details related to the standard curves and RT-PCR conditions were described in our previous study [9]. All samples were run in triplicate. The triplicate DNA extracts from each triplicate reactors were averaged out. The results were expressed as concentrations of gene copy number, which were normalized to 1 ng of DNA template, versus concentrations of nanomaterials.

2.4. 16S rRNA metagenomics sequencing

Metagenomics of sludge samples from reactors with and without G and GO were investigated using Illumina Miseq (Genome Sciences, Bioscience Division, Los Alamos National Laboratory,

New Mexico). The 16S rRNA gene libraries for each sample were prepared as described by Illumina with only modifications in the PCR amplification procedure. The conserved region targeted for analysis was the V4 region of the 16S rRNA gene using the primers F515 and R806 with Illumina adapters and barcodes [14]. More details on the library preparation and analysis can be found in the supporting information. Pair-end sequencing was employed using 600 - cycle MiSeq® Reagent Kit V3 (Illumina, U.S.A.). The output results from sequencing were analyzed using Ilumina basespace 16S Metagenomics v1.0.1. The data of metagenomics were deposited on the NCBI database under accession number SRP082429.

3. Results and discussions

3.1. Impact of graphene and graphene oxide on chemical parameter of the wastewater treatment

In a conventional wastewater treatment, Chemical oxygen demand (COD) removal is used as a mean to determine the treatment quality of biological processes. The results showed that COD removal reduced significantly after five and half days feeding the reactors with 1 mg L^{-1} GO and after three days feeding with 5 mg L^{-1} GO (Figure 1). We could estimate that there were about 3.64 mg L^{-1} (5.5 days) and 12.83 mg L^{-1} (3 days) GO in the reactors, respectively. These concentrations were the results of nanomaterial accumulation in the activated sludge due to the continuous feeding of nanomaterials in the influent (Figure S2). Consequently, the COD of the effluent in the 1 and 5 mg L^{-1} GO reactors were about 92 mg L^{-1} (5.5 days) and 78 mg L^{-1} (3 days), as opposed to 10 mg L^{-1} in the control reactors. In the case of G, significant reduction on the COD removal happened after 7.5 and 5.5 days for the reactors fed with 1 and 5 mg L^{-1} G, respectively (Figure 1). The reactors with both G and GO, after the initial and abrupt reduction in the COD removal, they reached a steady COD removal state. Overall, these results showed that lower nanomaterial input, *i.e.* 1 mg L^{-1}, led to less impact and smaller reduction on the COD

removal. Additionally, the fact that the COD removal reached a steady state and did not get completely stalled, suggested that some microbes could have been metabolic active in the presence of G and GO. Therefore, the impact of G and GO in the microbial metabolic activity was confirmed using the metabolic assay and Live and Dead staining (Figure 2 and S3). The results showed that the reactors exposed to the nanomaterials presented reduced metabolic activities than the controls and that several, but not all, cells were dead in these reactors, which explain the reduced removal of COD in the reactors with nanomaterials.

The impacts on COD removals in activated sludge were previously reported with other carbon based nanomaterials in long and short term assays [6, 7, 9]. For instance, acute toxicity studies with MWCNT and graphene agreed with each other that low concentrations (1 mg L^{-1}) of these nanomaterials for short time did not impact COD removal [7, 9]. In our study, the chronic toxicity, where the reactors were continuously fed with 1 mg L^{-1} of nanomaterials for several days, showed that the nanomaterials impact COD removal. These results were not observed in the chronic toxicity study with 1 mg L^{-1} MWCNT [7]. Clearly, different nanomaterials will present different toxic behaviors, this was more evident with our GO and G reactors, since the impact on COD removals were lower for G than for GO at each corresponding time, even though the accumulation of G in the sludge was higher than GO (Figure 1 and S2). These results show that GO tends to impact more the COD removal because of its higher antimicrobial properties than G, as previously described [15-17]. Overall G and GO impacted the COD in biological treatment, it is highly possible that these nanomaterials might affect as well as the microbial communities involved in specific nutrient removals, such as ammonia and phosphate.

3.2. Impact of chronic toxicity of G and GO on the wastewater biological process

Nitrogen and phosphorus are the two most important nutrients typically removed in the aerobic biological wastewater treatment process. These nutrients are essential to organisms, but if in excess, they are also responsible for causing serious environmental problems [18]. The aeration process helps in the removal of these pollutants in the form of ammonia (NH_3-N) and phosphate (PO_4^{3-}). In the present study, after 4 to 4.5 days, the reactors with 5 mg L^{-1} GO started to show reduced removals of ammonia and phosphate compared to the control reactors. While the 1 mg L^{-1} G and GO reactors took about 7 to 8.5 days, respectively, to start showing changes in nutrient removal. The 5 mg L^{-1} G reactor also showed an impact in the ammonia removal after four days, but not in the phosphate removal, which took about six and half days (Figure 3 and 5). The production of nitrate correlated well with the ammonia oxidation results (Figure 3 and 4), which showed that less nitrate from ammonia oxidation was being produced. Overall, the 5 mg L^{-1} GO reactors were the ones with the most pronounced effects on nutrient removal. Based on the mass balance results of the 5 mg L^{-1} reactors, after four days running the reactors, there was about 14.08 mg L^{-1} of GO accumulated in the sludge as opposed to 16.68 mg L^{-1} of G. The ammonia concentrations in the effluents at four days were 9.5 and 11.6 mg L^{-1} for 5 mg L^{-1} G and GO, respectively, while it was 0.2 mg L^{-1} for the control.

Even though there was more G accumulated in the sludge than GO, the reactors containing GO were the most affected. Previous studies have shown that microorganisms are more sensitive to GO than G [16, 17]. This sensitivity of microorganisms to GO was explained by the hydrophilic nature and the presence of functional groups in GO. Functional groups make the nanomaterial more prone to interact with biomacromolecules, heavy metals and other contaminants in the water [19, 20]. These bio-interactions could explain the higher toxic effects of GO to the sludge microbial community as compared to G. Additionally, other studies showed

that the presence of functional groups in GO led to the production of more reactive oxygen species, which is responsible for generating oxidative stress in microorganisms and cellular inactivation [6]. On the other hand, G is more hydrophobic and tends to aggregate in aqueous solutions, which explained the higher accumulation in sludge. These aggregates probably reduced the direct contact of G with microorganisms and therefore reduced its toxicity in the sludge. The large aggregates of G were also confirmed by microscopic observations (Figure S4).

In the reactors, concentrations of G and GO as low as 5.68 and 3.48 mg L^{-1}, respectively, started to affect the removal of ammonia and phosphate (1 mg L^{-1} nanomaterials reactors). The inhibition was more pronounced in concentrations as high as 16.68 and 14.08 mg L^{-1} for G and GO, respectively, in the 5 mg L^{-1} nanomaterials reactors (Figure S2). It is important to point out that even though the concentration of these nanomaterials continued to accumulate in the sludge from the influent, the removal of the nutrients still occurred in a steady manner, but with a lower performance than the control reactors (Figure 3 and 5). It is possible that a subset of the AOB and PAO populations or certain species in these populations could have been resistant and survived in the presence of these nanomaterials. These resistant populations were probably able to continue to perform the removal of nutrients in the sludge.

These hypotheses were further investigated with the quantification of AOB and PAO in the sludge. We quantified the AOB and PAO populations in the reactors using specific 16S rRNA genes for AOB, PAO and the functional gene ammonia monooxygenase (*amoA*) [21, 22]. Significant reduction in the PAO and AOB gene abundances were observed after four days for 5 mg L^{-1} of GO reactors (Figure 6 and 7), which corresponded to the lowest phosphate and ammonia removal in all the reactors (Figure 3 and 5). In the case of the 1 mg L^{-1} reactors, there

were also changes in the AOB and PAO populations after eight days, which matched the period where there were changes in the nutrient removals in these reactors.

It was, however, observed that the AOB and PAO populations slowly recovered after eight days running the reactor (Figure 6 and 7). This was corroborated by the fact that the abundance of the AOB population increased from 83 to 110 gene copies ng^{-1} for G and 37 to 90 gene copies ng^{-1} for GO in the 5 mg L^{-1} reactors between six and ten days (Figure 6a). While the PAO populations increased from 7.0 x 10^3 to 8.5 x 10^3 gene copies ng^{-1} for G and 6.9 x 10^3 to 9.8 x 10^3 gene copies ng^{-1} for GO in the 1 mg L^{-1} reactors between eight and ten days (Figure 7). The PAO population also increased in the reactor 5 mg L^{-1} GO from 5.6 x 10^3 to 9.5 x 10^3 gene copies ng^{-1}. Interestingly, the PAO increase only occurred in 1 mg L^{-1} G reactors, but not in the 5 mg L^{-1} G reactors. This was not the case for the AOBs. These results suggest that the PAO is probably much more sensitive to G than AOB. This sensitivity was also clearly seen by an earlier removal reduction of phosphate nutrients than the ammonia removal, even at low nanomaterial feeding concentrations, *i.e.* 1 mg L^{-1} for both G and GO (Figure 3 and 5). This difference could be due to the different and diverse bacterial composition in each group. In the case of PAO, *Betaproteobacteria* microorganisms are commonly involved in phosphate removal; while AOB is composed by both *Beta-* and *Gamma-proteobacteria* microorganisms [23, 24]. Although we observed a slightly increase in the AOB and PAO populations, the removal of ammonia and phosphate did not improve over time. It is possible that the AOB and PAO populations require more time to recover from the increasing accumulation of nanomaterials in the sludge. In Chen's study with copper nanoparticles, the phosphorous removal recovered over time, but the PAO population changed dramatically [25]. The authors described that other PAO, more resistant to copper, took over and continued to remove the nutrients. In addition to copper nanoparticles,

other studies with silver nanoparticles in activated sludge also showed similar trends. In these studies, the activity of both AOB and PAO populations were found to reach the same removal efficiency as their controls after 4 to 40 days [25-27]. Therefore, it is possible that the microbial community functionality in the wastewater can recover in the presence of G or GO. The long recovery time is probably due to the slow growth rates of these two populations [24, 28].

It is also worth point out that the inhibition of nitrogen and phosphate removals was previously reported in acute studies with carbon nanotubes and GO, but it is the first time that chronic toxicity is investigated with these nanomaterials. This study overall agrees with the fact that increasing concentrations of nanomaterials can impact the removal of ammonia and phosphate by affecting the AOB and PAO populations present in the sludge [6, 7]. In Hai's study, the authors showed that the microbial population was not able to adapt and recover overtime from the high initial dose (20 mg L^{-1}) of nanomaterials [7]. In our study, we saw signs of recovery of the AOB and PAO populations in the reactors after eight days, but these populations did not recover completely to allow satisfactory nutrient removal from the influent. It is possible, that giving more time to these populations, they could have fully recovered from the presence of these carbon-based nanomaterials. In the case of *amoA*, it is worth to note that the increase of *amoA* gene from eight to ten days was observed in 1mg L^{-1} GO and 5 mg L^{-1} G reactors only, which corroborates the results observed earlier with AOB (Figure S5).

Based on these results, these nanomaterials seem to also hold antimicrobial properties against nitrifiers and PAO in activated sludge, at least to some species belonging to these groups. The initial introduction of toxic materials, such as G and GO, agreed well with other studies for toxicity of nanomaterials to biological process. In these studies, the addition of nanomaterials led to suboptimum wastewater treatment in the bioreactors [31, 32]. In some cases, the microbial

community was able to recover and in others not [33]. In our study, we did deep sequencing investigations of the population exposed or not to nanomaterials to determine whether the microbial community in the sludge was adapting or other more resistant species were being selected and enriched in the presence of these nanomaterials.

3.4. Changes in the sludge microbial community exposed to graphene or graphene oxide

The changes in the microbial population structure after ten days exposed or not to the nanomaterials were analyzed using deep sequencing 16S rRNA to understand the chronic toxicity of these nanomaterials. The relative abundances of the phyla in all the reactors are shown in figure S6. The four most abundant phyla observed in the reactors were *Bacteroidetes*, *Proteobacteria*, *Firmicutes* and *Verrucomicrobia*. These phyla are commonly found in activated sludge of wastewater treatment plants [34]. In the reactors containing G and GO, there was a clear shift on these phyla. Also, the diversity of the reactors with nanomaterials decreased compared to the control reactor. The reactor presenting the lowest diversity was 5 mg L^{-1} GO (Table S2). The presence of G in the reactors led to increase in the *Bacteroidetes* population; while the GO reactors, enriched microbial populations from the *Proteobacteria* phylum. These results indicate that G and GO do not impact the same populations in the activated sludge.

At the genus level, the microbial communities in the different reactors containing nanomaterials changed significantly compared to the control reactor (Figure 8). Several genera that were found in the control reactors either disappeared or reduced to below the detection limit of the sequencing analysis in the GO and G reactors. That was the case for *Lewinella, Zoogloea, Dechloromonas*, *Candidatus Accumulibacter, Runella, Curvibacter*, *Thauera* and *Thermomonas* that are well-known microorganisms playing an essential role in biological wastewater treatment processes.

Lewinella, for instance, was described to biodegrade organic matter and hydrocarbons [35]. The reduction of this genus could have affected the removal of COD, as observed in our reactors. *Zoogloea* is another important genus for wastewater treatment that has the capability in helping the formation of sludge flocs and also reducing nitrate in wastewater [36-38]. The consequences of the reduction of this population could have yielded poor sludge flocculation and inefficient nitrogen removal in the wastewater. Another microorganism involved in nitrogen removal that also presented reduced abundance in the sludge containing G and GO was *Thauera.* This microorganism plays an important role in denitrification and removal of organic matter in wastewater [39-41]. *Thermomonas* was also shown to be a denitrifier in a full-scale wastewater treatment plant and in petroleum contaminated soil [42, 43]. The reduction of these populations has clearly reflected in the nitrogen and COD removals of the reactors.

In the case of the phosphate removal, *Dechloromonas, Runella* and *Candidatus Accumulibacter* play an essential role in phosphate removal in wastewater [44-48]. *Runella* has also been shown to improve formation of granular sludge [49]. The reduction of the PAO gene copy in the GO and G reactors could be explained by the reduction in these populations in the activated sludge. In addition to these microbes, *Dechloromonas* and *Curvibacter* were affected by the presence of G and GO. These two genera were reported in a previous study to reduce perchlorate in biological treatment, so they can also play a role in the wastewater treatment [50]. It is worth to note that the reduction of *Lewinella, Zoogloea, Dechloromonas*, *Curvibacter*, *Thermomonas* and *Flavobacterium* in this study was also observed in an acute toxicity study with graphene in activated sludge [9]. These results confirm that these populations are really sensitive to the presence of GO and G nanomaterials.

Even though some important groups of microorganisms involved in biological wastewater treatment were affected by the presence of G and GO, the results show that some populations were not as sensitive to the presence of these nanomaterials (Figure 8). It is important to point out that not the same groups of microorganisms were enriched in the G and GO reactors, as compared to the control reactors. For instance, in the G reactor, *Olivibacter*, *Haliangium* and *Dokdonella* were enriched, while in the GO reactor *Chryseobacterium*, *Pseudomonas, Stenotrophomonas*, *Acinetobacter*, *Brevundimonas* and *Pseudoxanthomonas* were the ones enriched (Figure 8). Some of these microorganisms have also been described to be involved in nutrient removal in wastewater. Specifically, *Olivibacter*, *Haliangium* and *Pseudoxanthomonas* were reported dominantly in nitrogen removal in which they were isolated from cow manure, biofilters for hydrocarbon clean-up, and full scale denitrification and granular sludge [42, 51, 52]. *Stenotrophomonas* and *Chryseobacterium* were not directly associated to nutrient removal in wastewater treatment plants, but they have been reported in previous studies to be important in nitrogen cycling and to dominate in biofilm reactors treating ammonia contaminated air [53, 54]. *Dokdonella*, *Pseudomonas* and *Acinetobacter* have been described to have the capability of accumulating phosphate. These genera were isolated and identified from phosphate removal activated sludge processes [55-57]. Hence, they play essential roles in nutrient removal in activated sludge. These genera did not seem to be impacted by the presence of the nanomaterials and were probably able to continue to remove the nutrients in the reactor, but since their cell concentrations were low, they were not able to remove the nutrients with the same efficiency as the original microbial populations in the sludge. These results would explain the observed increase in PAO and AOB populations in the RT-PCR analyses and the observed steady nutrient removal in the bioreactors during continuous additions of nanomaterials.

4. Conclusion

In conclusion, the accumulation of G and GO overtime resulted in a transient, but significant impact in the ability of the activated sludge to remove COD, ammonia and phosphate. G and GO concentrations starting to impact the wastewater treatment were as low as 5.26 mg L^{-1} and 3.64 mg L^{-1}, respectively. These concentrations correspond to the accumulation of G and GO in the sludge from 1 mg L^{-1} influent. The reactors receiving 5 mg L^{-1} influent resulted in higher and faster accumulation of G and GO in the sludge, which generated higher impacts in the biological wastewater treatment. It was noticeable that GO was more toxic than G, since GO is more hydrophilic and therefore aggregates less in the sludge; and because GO is more reactive toward biomolecules than G. The results also showed that the PAO and AOB community started to recover after eight days; however, there was a shift in the microbial community structure and diversity at end of ten days. These results suggest that some microbial communities in the sludge are less sensitive to the presence of these nanomaterials. Also, the different toxicity mechanisms of G and GO led to the selection of completely different populations of microorganisms in each reactor.

ACKNOLEDGEMENTS

This project was supported by the NSF Career Award Nanohealth # 104093.

SUPPORTING INFORMATION

Additional figures, tables and more discussions can be found in supporting information.

References

[1] E.J. Siochi, Graphene in the sky and beyond, Nat Nano, 9 (2014) 745-747.

[2] A.K. Geim, K.S. Novoselov, The rise of graphene, Nat Mater, 6 (2007) 183-191.

[3] S.C. Smith, D.F. Rodrigues, Carbon-based nanomaterials for removal of chemical and biological contaminants from water: A review of mechanisms and applications, Carbon, 91 (2015) 122-143.

[4] M.M. Gagliardi, A.; Moran, R., Graphene: Technologies, Applications, and Markets, in, BCC Research Market Forecasting, Wellesley, MA, 2012.

[5] A.A. Keller, A. Lazareva, Predicted Releases of Engineered Nanomaterials: From Global to Regional to Local, Environmental Science & Technology Letters, 1 (2014) 65-70.

[6] F. Ahmed, D.F. Rodrigues, Investigation of acute effects of graphene oxide on wastewater microbial community: A case study, Journal of hazardous materials, 256 (2013) 33-39.

[7] R. Hai, Y. Wang, X. Wang, Z. Du, Y. Li, Impacts of multiwalled carbon nanotubes on nutrient removal from wastewater and bacterial community structure in activated sludge, PloS one, 9 (2014) e107345.

[8] A. Parise, H. Thakor, X. Zhang, Activity inhibition on municipal activated sludge by single-walled carbon nanotubes, Journal of Nanoparticle Research, 16 (2013) 1-9.

[9] H.N. Nguyen, S.L. Castro, D.F. Rodrigues, Acute toxicity of Graphene Nanoplatelets on Biological Wastewater Treatment Process, Environmental Science: Nano, (2017).

[10] Y. Yang, Z. Yu, T. Nosaka, K. Doudrick, K. Hristovski, P. Herckes, P. Westerhoff, Interaction of carbonaceous nanomaterials with wastewater biomass, Frontiers of Environmental Science & Engineering, 9 (2015) 823-831.

[11] W.S. Hummers, R.E. Offeman, Preparation of Graphitic Oxide, Journal of the American Chemical Society, 80 (1958) 1339-1339.

[12] H.N. Nguyen, S.L. Castro-Wallace, D.F. Rodrigues, Acute toxicity of graphene nanoplatelets on biological wastewater treatment process, Environmental Science: Nano, 4 (2017) 160-169.

[13] J.V.D. Perez, E.T. Nadres, H.N. Nguyen, M.L.P. Dalida, D.F. Rodrigues, Response Surface Methodology as a powerful tool to optimize the synthesis of polymer-based graphene oxide nanocomposites for simultaneous removal of cationic and anionic heavy metal contaminants, RCS advance, DOI: 10.1039/c7ra00750g. (2017).

[14] E. Singer, B. Bushnell, D. Coleman-Derr, B. Bowman, R.M. Bowers, A. Levy, E.A. Gies, J.-F. Cheng, A. Copeland, H.-P. Klenk, S.J. Hallam, P. Hugenholtz, S.G. Tringe, T. Woyke, High-resolution phylogenetic microbial community profiling, ISME J, (2016).

[15] I.E. Mejias Carpio, C.M. Santos, X. Wei, D.F. Rodrigues, Toxicity of a polymer-graphene oxide composite against bacterial planktonic cells, biofilms, and mammalian cells, Nanoscale, 4 (2012) 4746-4756.

[16] S. Liu, T.H. Zeng, M. Hofmann, E. Burcombe, J. Wei, R. Jiang, J. Kong, Y. Chen, Antibacterial Activity of Graphite, Graphite Oxide, Graphene Oxide, and Reduced Graphene Oxide: Membrane and Oxidative Stress, ACS Nano, 5 (2011) 6971-6980.

[17] C.M. Santos, J. Mangadlao, F. Ahmed, A. Leon, R.C. Advincula, D.F. Rodrigues, Graphene nanocomposite for biomedical applications: fabrication, antimicrobial and cytotoxic investigations, Nanotechnology, 23 (2012) 395101.

[18] H.W. Paerl, L.M. Valdes, A.R. Joyner, M.F. Piehler, M.E. Lebo, Solving Problems Resulting from Solutions: Evolution of a Dual Nutrient Management Strategy for the Eutrophying Neuse River Estuary, North Carolina, Environmental Science & Technology, 38 (2004) 3068-3073.
[19] S.C. Smith, F. Ahmed, K.M. Gutierrez, D. Frigi Rodrigues, A comparative study of lysozyme adsorption with graphene, graphene oxide, and single-walled carbon nanotubes: Potential environmental applications, Chemical Engineering Journal, 240 (2014) 147-154.
[20] G. Zhao, J. Li, X. Ren, C. Chen, X. Wang, Few-Layered Graphene Oxide Nanosheets As Superior Sorbents for Heavy Metal Ion Pollution Management, Environmental Science & Technology, 45 (2011) 10454-10462.
[21] M. Bellucci, T.P. Curtis, Chapter Eleven - Ammonia-Oxidizing Bacteria in Wastewater, in: G.K. Martin, Y.S. Lisa (Eds.) Methods in Enzymology, Academic Press, 2011, pp. 269-286.
[22] A. Oehmen, G. Carvalho, C.M. Lopez-Vazquez, M.C.M. van Loosdrecht, M.A.M. Reis, Incorporating microbial ecology into the metabolic modelling of polyphosphate accumulating organisms and glycogen accumulating organisms, Water Research, 44 (2010) 4992-5004.
[23] R.P.X. Hesselmann, C. Werlen, D. Hahn, J.R. van der Meer, A.J.B. Zehnder, Enrichment, Phylogenetic Analysis and Detection of a Bacterium That Performs Enhanced Biological Phosphate Removal in Activated Sludge, Systematic and Applied Microbiology, 22 (1999) 454-465.
[24] W. Martens-Habbena, P.M. Berube, H. Urakawa, J.R. de la Torre, D.A. Stahl, Ammonia oxidation kinetics determine niche separation of nitrifying Archaea and Bacteria, Nature, 461 (2009) 976-979.
[25] H. Chen, X. Li, Y. Chen, Y. Liu, H. Zhang, G. Xue, Performance of wastewater biological phosphorus removal under long-term exposure to CuNPs: adapting toxicity via microbial community structure adjustment, RSC Advances, 5 (2015) 61094-61102.
[26] Y. Wang, Y. Zhao, M. Ji, H. Zhai, Nitrification recovery behavior by bio-accelerators in copper-inhibited activated sludge system, Bioresour Technol, 192 (2015) 748-755.
[27] C.L. Alito, C.K. Gunsch, Assessing the Effects of Silver Nanoparticles on Biological Nutrient Removal in Bench-Scale Activated Sludge Sequencing Batch Reactors, Environmental Science & Technology, 48 (2014) 970-976.
[28] M. Sidat, F. Bux, H. Kasan, Polyphosphate accumulation by bacteria isolated from activated sludge, Water Sa, 25 (1999) 175-179.
[29] S. Bykkam, K. Rao, C. Chakra, T. Thunugunta, Synthesis and characterization of graphene oxide and its antimicrobial activity against klebseilla and staphylococus, Int. J. Adv. Biotechnol. Res, 4 (2013) 142.
[30] O. Akhavan, E. Ghaderi, Toxicity of graphene and graphene oxide nanowalls against bacteria, Acs Nano, 4 (2010) 5731-5736.
[31] G. Bystrzejewska-Piotrowska, J. Golimowski, P.L. Urban, Nanoparticles: Their potential toxicity, waste and environmental management, Waste Management, 29 (2009) 2587-2595.
[32] B. Sundaram, A. Kumar, Toxicity of a Mixture of Metal Oxide Nanoparticles on Activated Sludge, in: Emerging Micro-Pollutants in the Environment: Occurrence, Fate, and Distribution, American Chemical Society, 2015, pp. 149-165.
[33] Y. Ma, J.W. Metch, E.P. Vejerano, I.J. Miller, E.C. Leon, L.C. Marr, P.J. Vikesland, A. Pruden, Microbial community response of nitrifying sequencing batch reactors to silver,

zero-valent iron, titanium dioxide and cerium dioxide nanomaterials, Water Research, 68 (2015) 87-97.
[34] L. Ye, T. Zhang, Bacterial communities in different sections of a municipal wastewater treatment plant revealed by 16S rDNA 454 pyrosequencing, Appl Microbiol Biotechnol, 97 (2013) 2681-2690.
[35] R.M.M. Abed, S. Al-Kharusi, S. Prigent, T. Headley, Diversity, Distribution and Hydrocarbon Biodegradation Capabilities of Microbial Communities in Oil-Contaminated Cyanobacterial Mats from a Constructed Wetland, PLoS ONE, 9 (2014) e114570.
[36] A. Cydzik-Kwiatkowska, M. Zielińska, Bacterial communities in full-scale wastewater treatment systems, World Journal of Microbiology & Biotechnology, 32 (2016) 66.
[37] Z. Yu, W.W. Mohn, Bioaugmentation with the resin acid-degrading bacterium Zoogloea resiniphila DhA-35 to counteract pH stress in an aerated lagoon treating pulp and paper mill effluent, Water Research, 36 (2002) 2793-2801.
[38] Y. Shao, B.S. Chung, S.S. Lee, W. Park, S.-S. Lee, C.O. Jeon, Zoogloea caeni sp. nov., a floc-forming bacterium isolated from activated sludge, International Journal of Systematic and Evolutionary Microbiology, 59 (2009) 526-530.
[39] B. Liu, F. Zhang, X. Feng, Y. Liu, X. Yan, X. Zhang, L. Wang, L. Zhao, Thauera and Azoarcus as functionally important genera in a denitrifying quinoline-removal bioreactor as revealed by microbial community structure comparison, FEMS Microbiol Ecol, 55 (2006) 274-286.
[40] Y. Zhao, J. Huang, H. Zhao, H. Yang, Microbial community and N removal of aerobic granular sludge at high COD and N loading rates, Bioresource Technology, 143 (2013) 439-446.
[41] Q. Ma, Y. Qu, W. Shen, Z. Zhang, J. Wang, Z. Liu, D. Li, H. Li, J. Zhou, Bacterial community compositions of coking wastewater treatment plants in steel industry revealed by Illumina high-throughput sequencing, Bioresource Technology, 179 (2015) 436-443.
[42] S.J. McIlroy, A. Starnawska, P. Starnawski, A.M. Saunders, M. Nierychlo, P.H. Nielsen, J.L. Nielsen, Identification of active denitrifiers in full-scale nutrient removal wastewater treatment systems, Environ Microbiol, 18 (2016) 50-64.
[43] S.C. de la Cueva, C.H. Rodríguez, N.O.S. Cruz, J.A.R. Contreras, J.L. Miranda, Changes in Bacterial Populations During Bioremediation of Soil Contaminated with Petroleum Hydrocarbons, Water, Air, & Soil Pollution, 227 (2016) 1-12.
[44] J. Ahn, S. Schroeder, M. Beer, S. McIlroy, R.C. Bayly, J.W. May, G. Vasiliadis, R.J. Seviour, Ecology of the Microbial Community Removing Phosphate from Wastewater under Continuously Aerobic Conditions in a Sequencing Batch Reactor, Applied and Environmental Microbiology, 73 (2007) 2257-2270.
[45] S. Günther, M. Trutnau, S. Kleinsteuber, G. Hause, T. Bley, I. Röske, H. Harms, S. Müller, Dynamics of Polyphosphate-Accumulating Bacteria in Wastewater Treatment Plant Microbial Communities Detected via DAPI (4′,6′-Diamidino-2-Phenylindole) and Tetracycline Labeling, Applied and Environmental Microbiology, 75 (2009) 2111-2121.
[46] A. Copeland, X. Zhang, M. Misra, A. Lapidus, M. Nolan, S. Lucas, S. Deshpande, J.-F. Cheng, R. Tapia, L.A. Goodwin, S. Pitluck, K. Liolios, I. Pagani, N. Ivanova, N. Mikhailova, A. Pati, A. Chen, K. Palaniappan, M. Land, L. Hauser, C. Pan, C.D. Jeffries, J.C. Detter, E.-M. Brambilla, M. Rohde, O.D. Ngatchou Djao, M. Göker, J. Sikorski, B.J. Tindall, T. Woyke, J. Bristow, J.A. Eisen, V. Markowitz, P. Hugenholtz, N.C. Kyrpides, H.-P. Klenk, K.

Mavromatis, Complete genome sequence of the aquatic bacterium Runella slithyformis type strain (LSU 4T), Standards in Genomic Sciences, 6 (2012) 145-154.
[47] S. Lu, J.R. Lee, S.H. Ryu, B.S. Chung, W.-S. Choe, C.O. Jeon, Runella defluvii sp. nov., isolated from a domestic wastewater treatment plant, International Journal of Systematic and Evolutionary Microbiology, 57 (2007) 2600-2603.
[48] S.H. Ryu, T.T. Nguyen, W. Park, C.J. Kim, C.O. Jeon, Runella limosa sp. nov., isolated from activated sludge, International journal of systematic and evolutionary microbiology, 56 (2006) 2757-2760.
[49] N. Abdullah, A. Yuzir, T.P. Curtis, A. Yahya, Z. Ujang, Characterization of aerobic granular sludge treating high strength agro-based wastewater at different volumetric loadings, Bioresource Technology, 127 (2013) 181-187.
[50] X. Li, W. Yuen, E. Morgenroth, L. Raskin, Backwash intensity and frequency impact the microbial community structure and function in a fixed-bed biofilm reactor, Applied Microbiology and Biotechnology, 96 (2012) 815-827.
[51] S. Ntougias, A. Lapidus, J. Han, K. Mavromatis, A. Pati, A. Chen, H.-P. Klenk, T. Woyke, C. Fasseas, N.C. Kyrpides, G.I. Zervakis, High quality draft genome sequence of Olivibacter sitiensis type strain (AW-6(T)), a diphenol degrader with genes involved in the catechol pathway, Standards in Genomic Sciences, 9 (2014) 783-793.
[52] D.G. Weissbrodt, N. Shani, C. Holliger, Linking bacterial population dynamics and nutrient removal in the granular sludge biofilm ecosystem engineered for wastewater treatment, FEMS Microbiology Ecology, 88 (2014) 579-595.
[53] R.P. Ryan, S. Monchy, M. Cardinale, S. Taghavi, L. Crossman, M.B. Avison, G. Berg, D. van der Lelie, J.M. Dow, The versatility and adaptation of bacteria from the genus Stenotrophomonas, Nature Reviews. Microbiology, 7 (2009) 514-525.
[54] S. Gerrity, E. Clifford, C. Kennelly, G. Collins, Ammonia oxidizing bacteria and archaea in horizontal flow biofilm reactors treating ammonia-contaminated air at 10 °C, Journal of Industrial Microbiology & Biotechnology, 43 (2016) 651-661.
[55] G.W. Fuhs, M. Chen, Microbiological Basis of Phosphate Removal in the Activated Sludge Process for the Treatment of Wastewater, Microbial Ecology, 2 (1975) 119-138.
[56] L. Lötter, M. Murphy, The identification of heterotrophic bacteria in an activated sludge plant with particular reference to polyphosphate accumulation, Water S. A., 11 (1985) 179-184.
[57] B.-C. Kim, S. Kim, T. Shin, H. Kim, B.-I. Sang, Comparison of the Bacterial Communities in Anaerobic, Anoxic, and Oxic Chambers of a Pilot A2O Process Using Pyrosequencing Analysis, Current Microbiology, 66 (2013) 555-565.

Figure 1: Chemical oxygen demand in influent and effluent of the control and reactors treated with G and GO at different concentrations (1 and 5 mg L^{-1}). The error bars represent standard deviations from triplicate reactors.

Figure 2: The metabolic activity of effluent sludge from control and treated G or GO reactors in different concentrations at 10 days. The error bars represent standard deviations from triplicate reactors. (*) Shows statistically significant different results (t-test with $P \leq 0.05$).

Figure 3: Nitrogen residual as ammonia in influent and effluent for the control and reactors treated with G and GO at different concentrations. The error bars represent standard deviations from triplicate reactors.

Figure 4: Nitrogen residual as nitrate in influent and effluent for the control and reactors treated with G and GO at different concentrations. The error bars represent the standard deviation from triplicate reactors.

Figure 5: Phosphorus residual as phosphate in influent and effluent for the control and reactors treated with G and GO at different concentrations. The error bars represent the standard deviation from triplicate reactors.

Figure 6: Abundance of 16S rRNA ammonia oxidizing bacteria gene copies (AOB) in activated sludge, expressed as gene copy number normalized per nanogram of DNA.

Figure 7: Abundance of 16S rRNA phosphate accumulating bacterial (PAO) gene copies in activated sludge, expressed as gene copy number normalized per nanogram of DNA.

Figure 8: Heatmap of relative abundances of different genera in the reactors with and without G or GO. Color scale from Red (lowest abundance) to Green (highest abundance).

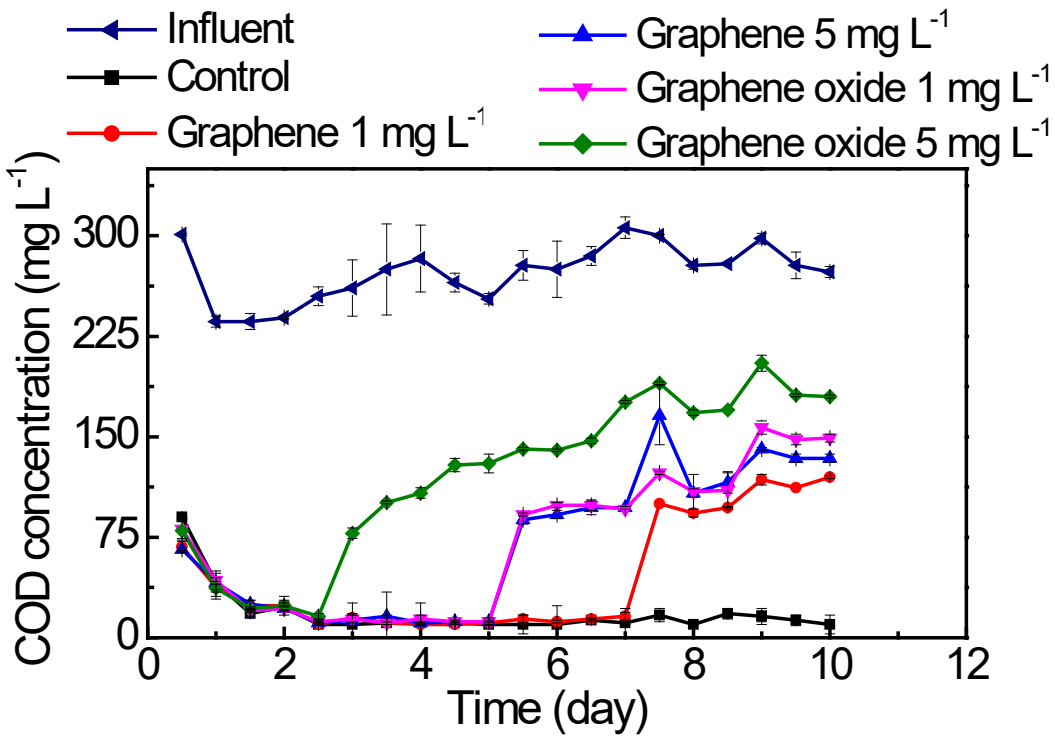
Influent
Control
Graphene 1 mg L-1
Graphene 5 mg L-1
Graphene oxide 1 mg L-1
Graphene oxide 5 mg L-1
COD concentration (mg L-1)
300
225
150
75
0
0
2
4
6
8
10
12
Time (day)

Figure 1

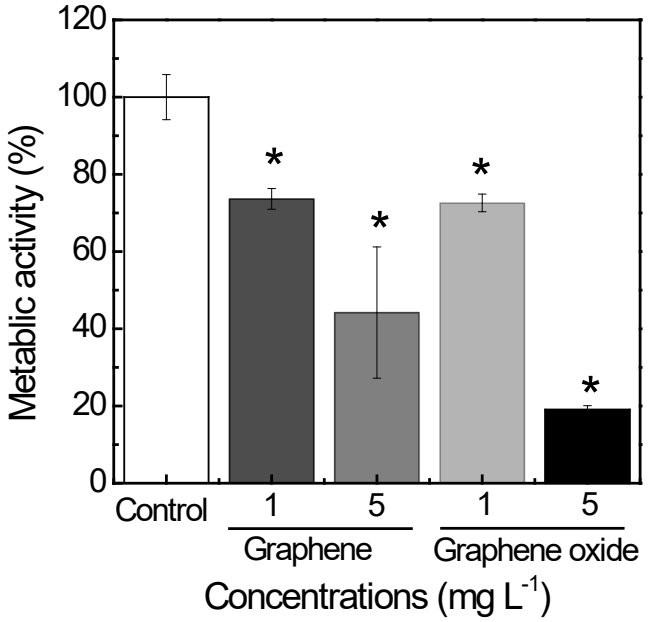
120
100
80
60
40
20
0
Metablic activity (%)
*
*
*
*
Control
1
5
1
5
Graphene
Graphene oxide
Concentrations (mg L-1)

Figure 2

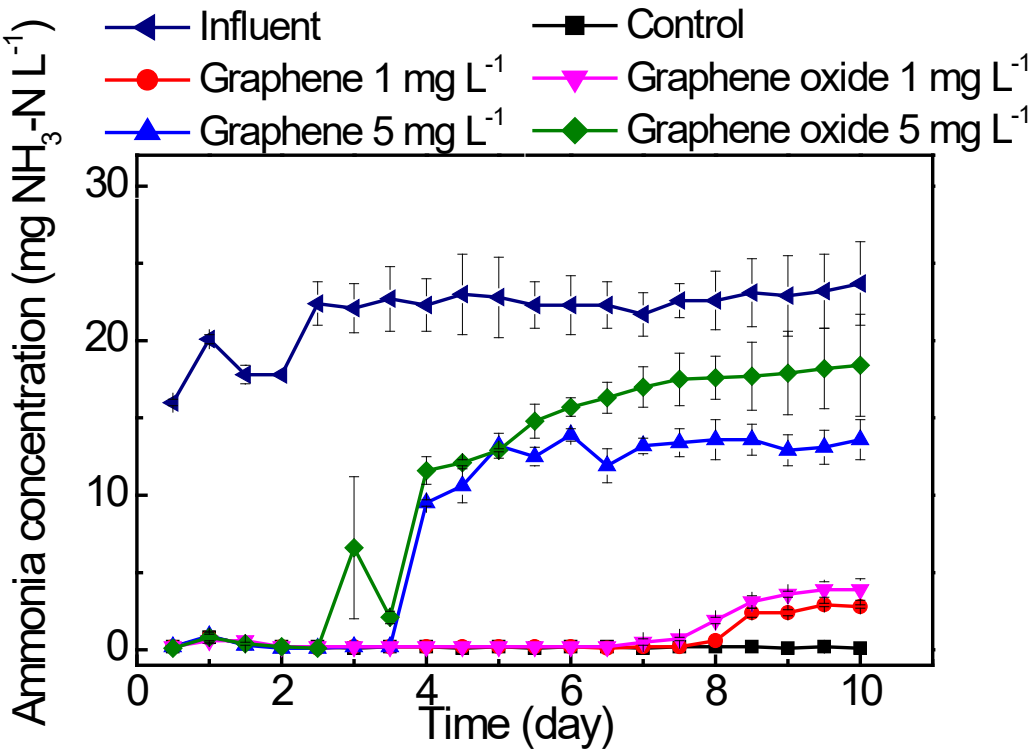
Influent
Control
Graphene 1 mg L-1
Graphene oxide 1 mg L-1
Graphene 5 mg L-1
Graphene oxide 5 mg L-1
Ammonia concentration (mg NH3-N L-1)
Time (day)
0
10
20
30
0
2
4
6
8
10

Figure 3

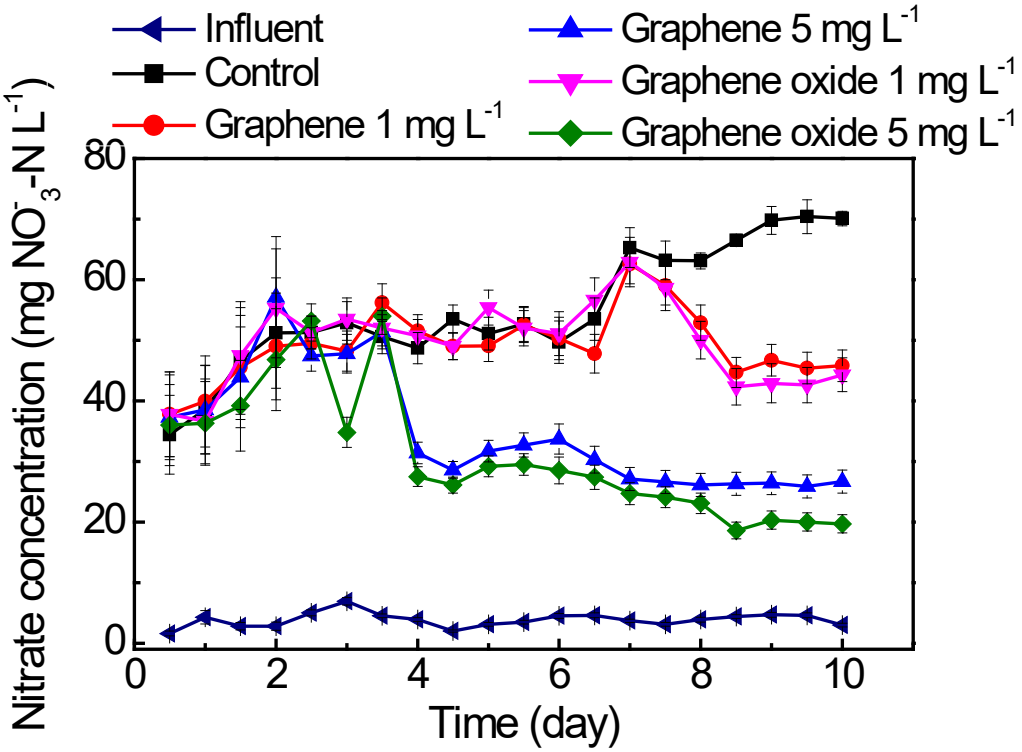
Influent
Control
Graphene 1 mg L-1
Graphene 5 mg L-1
Graphene oxide 1 mg L-1
Graphene oxide 5 mg L-1
Nitrate concentration (mg NO3--N L-1)
Time (day)
0
20
40
60
80
0
2
4
6
8
10

Figure 4

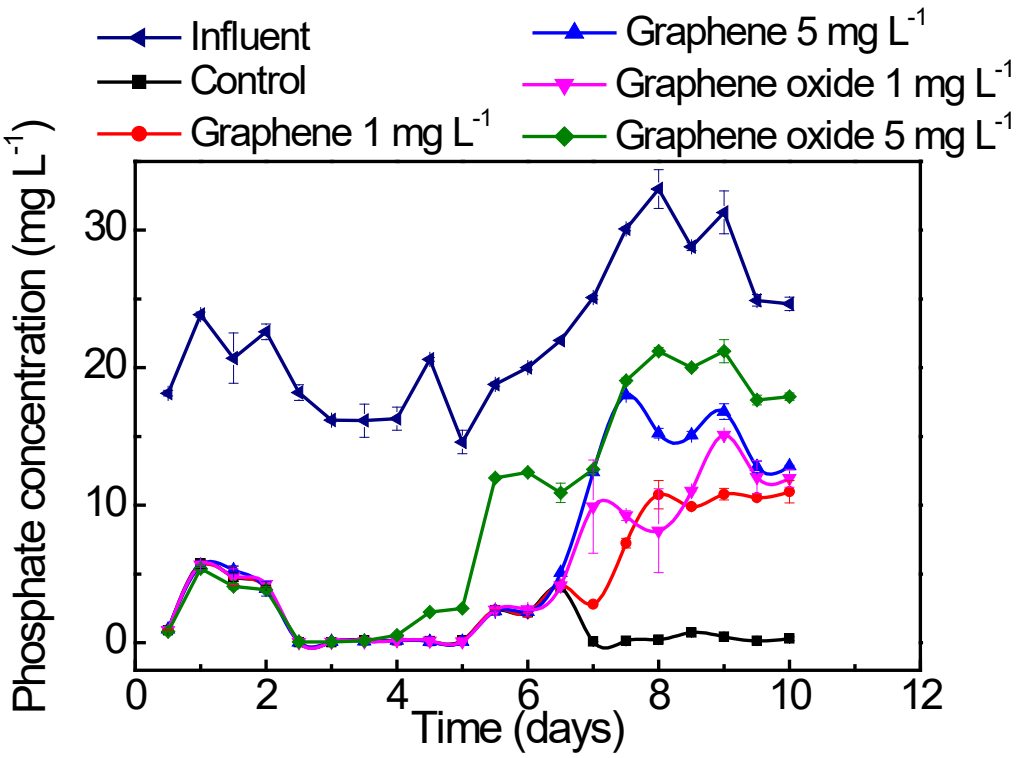
Influent
Control
Graphene 1 mg L-1
Graphene 5 mg L-1
Graphene oxide 1 mg L-1
Graphene oxide 5 mg L-1
Phosphate concentration (mg L-1)
Time (days)
0
10
20
30
0
2
4
6
8
10
12

Figure 5

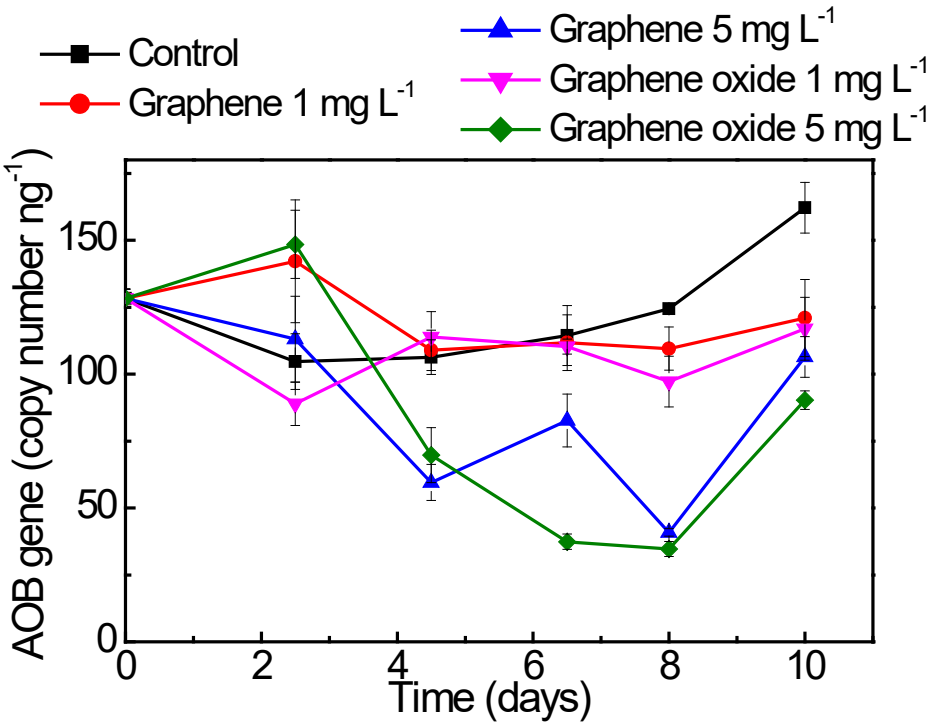
Control
Graphene 1 mg L-1
Graphene 5 mg L-1
Graphene oxide 1 mg L-1
Graphene oxide 5 mg L-1
AOB gene (copy number ng-1)
0
50
100
150
0
2
4
6
8
10
Time (days)

Figure 6

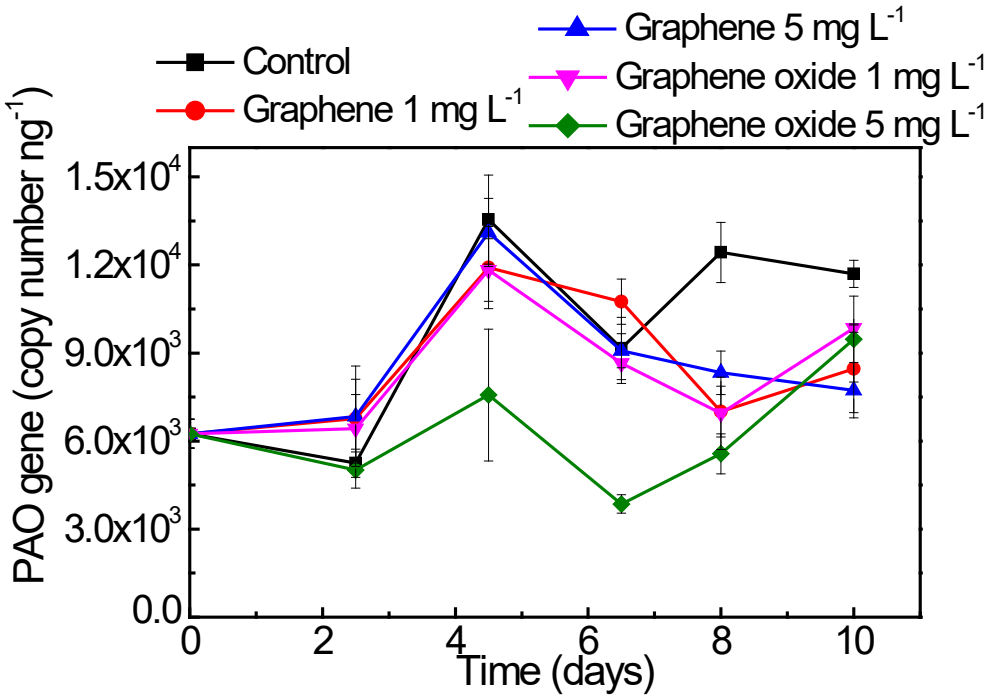
Control
Graphene 1 mg L-1
Graphene 5 mg L-1
Graphene oxide 1 mg L-1
Graphene oxide 5 mg L-1
PAO gene (copy number ng-1)
1.5x10^4
1.2x10^4
9.0x10^3
6.0x10^3
3.0x10^3
0.0
0
2
4
6
8
10
Time (days)

Figure 7

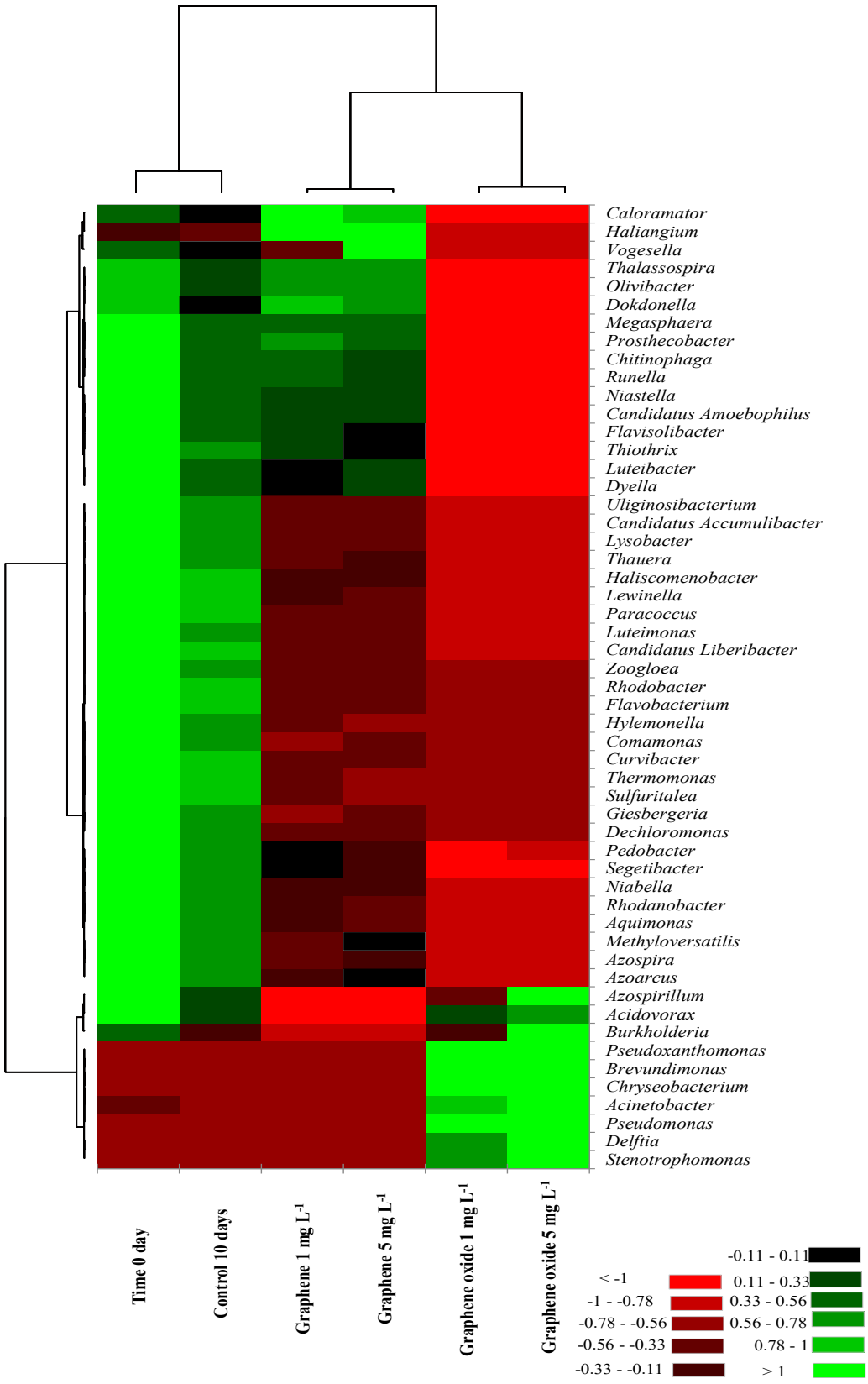
Caloramator
Haliangium
Vogesella
Thalassospira
Olivibacter
Dokdonella
Megasphaera
Prosthecobacter
Chitinophaga
Runella
Niastella
Candidatus Amoebophilus
Flavisolibacter
Thiothrix
Luteibacter
Dyella
Uliginosibacterium
Candidatus Accumulibacter
Lysobacter
Thauera
Haliscomenobacter
Lewinella
Paracoccus
Luteimonas
Candidatus Liberibacter
Zoogloea
Rhodobacter
Flavobacterium
Hylemonella
Comamonas
Curvibacter
Thermomonas
Sulfuritalea
Giesbergeria
Dechloromonas
Pedobacter
Segetibacter
Niabella
Rhodanobacter
Aquimonas
Methyloversatilis
Azospira
Azoarcus
Azospirillum
Acidovorax
Burkholderia
Pseudoxanthomonas
Brevundimonas
Chryseobacterium
Acinetobacter
Pseudomonas
Delftia
Stenotrophomonas
Time 0 day
Control 10 days
Graphene 1 mg L-1
Graphene 5 mg L-1
Graphene oxide 1 mg L-1
Graphene oxide 5 mg L-1
< -1
-1 - -0.78
-0.78 - -0.56
-0.56 - -0.33
-0.33 - -0.11
-0.11 - 0.11
0.11 - 0.33
0.33 - 0.56
0.56 - 0.78
0.78 - 1
> 1

Figure 8